Turkish Journal of Electrical Engineering & Computer Sciences

http://journals.tubitak.gov.tr/elektrik/

Research Article

Turk J Elec Eng & Comp Sci
(2016) 24: 2454 – 2468

doi:10.3906/elk-1312-198

An adaptive fuzzy PI controlled bus quantity enhancer for wave energy systems

Emre ÖZKOP[1,*], Adel Mahmoud SHARAF[2], İsmail Hakkı ALTAŞ[1]
[1]Department of Electrical and Electronics Engineering, Faculty of Engineering, Karadeniz Technical University, Trabzon, Turkey
[2]Sharaf Energy Systems, Inc., Fredericton, NB, Canada

Received: 24.12.2013 • **Accepted/Published Online:** 19.08.2014 • **Final Version:** 15.04.2016

Abstract: This paper introduces an adaptive fuzzy PI controller (AFPIC) for a flexible AC transmission system (FACTS)-based dynamic power filter (DPF) to be used in wave energy conversion systems. The new FACTS device stabilizes the DC-common bus voltage, reduces quality of power troubles, and enhances energy utilization by acting as a bus quantity enhancer (BQE). The design and realization of the proposed FACTS-based DPF and efficient control schemes are fully studied. To validate the efficiency of the proposed BQE FACTS device, a digital simulation model and a laboratory test system are developed in the MATLAB/Simulink/Simpower software environment for comparison. Various experimental test models of the proposed BQE system and dynamic error-based controller structures have been utilized to verify the simulation results. It has been shown that the utilization of the proposed AFPIC with the novel BQE device and multivariable error driven control strategy is very effective to eliminate stochastic wave influences on voltage on the load side and load variations on the source side by decreasing voltage sag and swells. The effectiveness of the BQE is also tested by applying error energy-based performance indices ISE, IAE, and ITAE.

Key words: Wave energy, power filter, FACTS, bus quantity enhancer, adaptive fuzzy PI control, multivariable error driven control

1. Introduction

Energy demand in the world has increased day by day because of the population expansion with economic growth. Nonrenewable energy sources supply over 80% of the energy demand of the world's population today [1,2]. Concerns about the environment and energy problems motivate people to seek alternative energy sources, which are more clean, balanced, sustainable, and reliable. Since there is no restraint in the sense of renewable resources, specialists foresee that the future belongs to renewable energy resources [3–5]. Many projects focusing on diverse renewable resources (solar, wind, wave, etc.) have been carried out [6,7]. Wave energy has key features such as energy in high density, less investment, low running cost, abundancy, wide availability, and a variety of ways to harness it so that it is an encouraging renewable energy source attracting investors currently [8–10]. Wave energy potential is estimated to be about 8000-80,000 TWh per year or 1–10 TW around the world, and wind and solar sources have 15–20 times less energy density (watt/m^2) than waves [9,10]. Wave energy can supply about 1%–5% of the world's annual electricity demand [11]. The extractable wave energy potential can substantially contribute to the world's electricity demand [9]. Conventional energy cost is about 5 times less than that of wave energy, but nonetheless wave energy costs can be competitive with that of conventional energy

*Correspondence: eozkop@ktu.edu.tr

if it is preferred as a base energy unit. Several commercial-scale projects on wave energy have been practically applied in some countries [8,9,12–14]. There are diverse techniques for wave energy conversion studied in the literature [15]. The stochastic feature of wave power conversion systems causes variable amplitudes and variable frequency in AC or DC voltage to supply the loads, which need constant magnitude/frequency on voltage. Thus, an interface device must be designed and applied to overcome undesirable effects of the waves.

Various types of power electronics interface topologies are used in wave energy conversion systems to provide the requirements between the energy system and load. In [16], DC/DC buck converter topologies were implemented to both charge the battery and supply loads. Electrical power was regulated by power electronics AC/DC/AC converters in [17,18]. AC/DC/AC and AC/DC converters were presented for active filtering in [19]. A D-STATCOM (distribution static synchronous compensator) device was adapted to smooth power oscillation in [20]. A three-phase active rectifier and buck converter were used to provide power flow through a load in [21]. In [22], an H-bridge and Miller's converter were considered to be installed in a wave energy conversion system. A three-phase full-wave passive rectifier circuit was proposed to utilize power from a wave energy converter in [23]. A 3-phase AC/AC converter was introduced to enable constant power flow with maximum energy conversion from a wave energy converter in [24], while in [25] a passive diode rectifier and a capacitor filter were used to get smoother power output. Four different topologies based on AC/DC/AC converters were discussed to determine the pros and cons for system performance in [26], and in [27] AC/DC/AC converters were applied including active or passive mode in the AC/DC stage with transformers to adjust maximum power transmission to the consumer. A half-controlled single-phase bridge circuit produced a DC output current from wave energy devices in [28]. A diode-clamped three-level inverter was proposed to reduce the voltage change range of wave energy generation systems in [29]. The power electronics interface devices mentioned above have superiorities in terms of high efficiency, low cost, high reliability, compliance with standards, smaller total harmonic distortion, and so on.

The power electronics interface needs to be managed with a control system to compensate variations observed in a wave energy system output, so the load side voltage can be more robust. Different control methods have been discussed in the literature [12,30,31].

The initial state of this paper was given in [32], in which only the classical PI controller was used without any performance analysis. The work in [32] has been extended to include a fuzzy tuning ability along with the performance analysis of the controller. Therefore, in this study, a fuzzy tuned adaptive PI controller is developed for a novel FACTS-based BQE [33] using a multivariable dynamic error driven regulator. The adaptive fuzzy tuned PI controller (AFTPIC) uses the output of multivariable dynamic total error signal and generates the required gating signals for the BQE, which acts as a power conditioner and as a voltage regulator for the wave energy conversion (WEC) system. A simulation model of the overall proposed system is developed in the MATLAB environment using Simulink blocks and verified by comparing the results with that from the laboratory prototype implementation model operating under similar conditions possible for different cases. The WEC system (WECS) performance is observed using a permanent magnet DC (PMDC) motor load driven by the DC-DC converter. The purpose of the adaptive fuzzy PI controlled FACTS BQE system is to ensure the efficient transfer of the wave energy gathered in the DC bus into the load side connected to the DC-DC converter at the arranged voltage and frequency.

The DC bus voltage is more stable by means of the controlled power interface device. The effectiveness of fuzzy logic PI-tuned parameters is also tested by applying error energy-based performance indices: the integral of squared error (ISE), integral of absolute error (IAE), and integral of time multiplied absolute error (ITAE).

The load demands are provided via the DC-DC buck converter control. A DC bus is established to provide a connection between the generation side output and load side input. The DC bus affects both generation and dissipation sides. The objective is to look into the WECS operational characteristics as the generating unit feeding the load. The simulation and experimental results are used to make the necessary comparisons between the study schemes so that an efficient WECS design can be realized owing to the results observed in this study.

This paper illustrates the validation of the effectiveness of the proposed novel FACTS bus quantity enhancer and fuzzy logic tuned PI controller for the wave energy utilization system. Since the decision on parameter tuning of the PI controller is made by a fuzzy logic algorithm based on desired and measured output information of the system, the tuning may also be called intelligent tuning.

The rest of the paper is organized as follows. The study of the system and its modeling are described in Section 2. Section 3 briefly presents novel control designs. In Section 4, a detailed system simulation model is given. The experimental laboratory prototype validation is described in Section 5. The simulations and experimental results are presented in Section 6. Finally, the conclusions are given in Section 7.

2. The wave energy conversion system

The energy utilization scheme for the WECS is shown in Figure 1a with the novel BQE. The unified system consists of a wave energy source, an AC/DC interface, a passive diode rectifier, a filter that is a novel power electronics interface called a BQE system, a DC-DC converter, and a DC motor as the load.

Since the wave has a stochastic nature, the wave generator output voltage is not completely periodic and it has variations and considerable oscillations. The wave energy converter output voltage with variable frequency and amplitude is regulated with a full wave rectifier to reduce undulation in the voltage and then the regulated voltage is transmitted to the DC power collection and distribution bus. It is an idea to use the common DC bus as a collection and distribution bus in order to gather power generated by other similar wave systems into one common bus instead of distributing it to loads. The common DC bus voltage is regulated by the BQE converter to obtain a more reliable and stable voltage waveform and transfer the power to a PMDC motor load through a buck converter. Effective control strategies for the switched power electronic devices, which are the BQE scheme and buck converter, are also enhanced within the context of the paper.

2.1. Wave energy generator

2.1.1. Mathematical model of the wave energy conversion

A generator is one of the main components of the WEC. Therefore, different types of generator technologies are proposed in the literature. A permanent magnet linear generator (PMLG) is modeled and used in consideration of the studies given in [34,35].

Real sea waves have randomness in height, period, and direction. This randomness can be simplified to a sinusoidal wave, which is an averaged periodical form of the random behavior of the actual waves. The periodical sine wave model given in Eqs. (1)–(4) is used in studies for simplicity [36,37] as is done here. The wave turbine and generator used in this study are designed to be used with regular wave characteristics of the Eastern Black Sea coast of Turkey. Since the system is planned to be used under normal weather conditions with regular wave characteristics excluding the extra high waves of windy conditions, a simplified periodical sine wave model is preferred. The wave characteristics used in model are represented by Eq. (1):

$$w_s = \frac{\pi H}{T} \sin(-\frac{2\pi}{T} t), \tag{1}$$

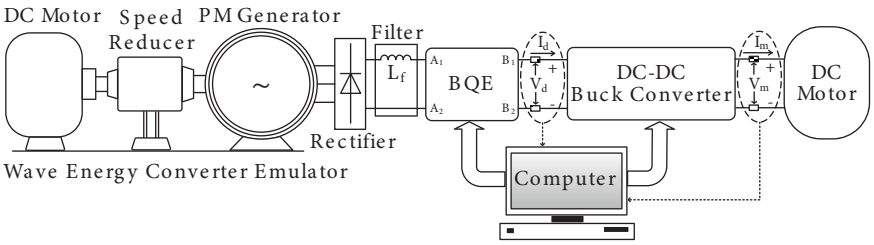

(a) WEC scheme-laboratory set-up with the BQE

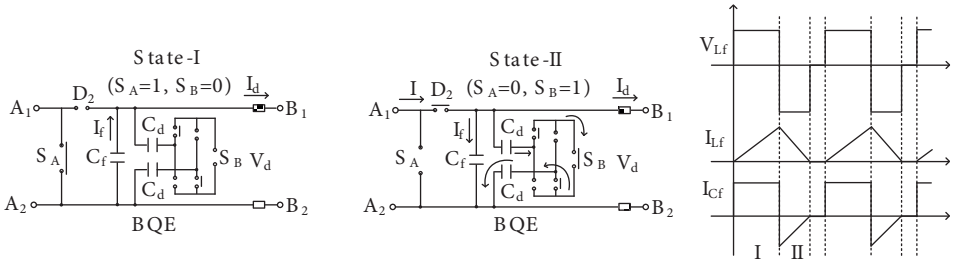

(b) Operating modes and switching waveforms of the BQE device

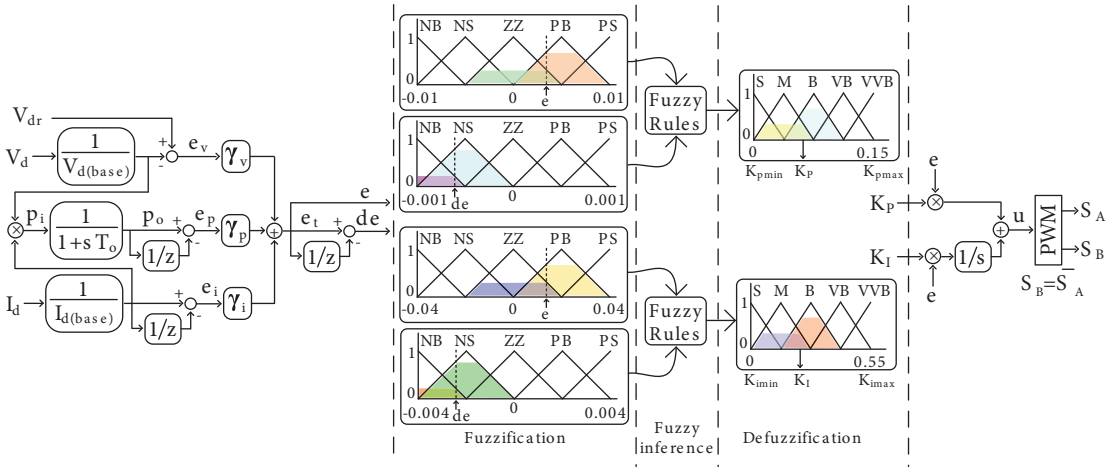

(c) Dynamic error driven multi-variable control scheme for the BQE

Figure 1. The system general block diagram. (a) WEC scheme: laboratory setup with the BQE. (b) Operating modes and switching waveforms of the BQE device. (c) Dynamic error driven multivariable control scheme for the BQE.

where T and H are wave period and height, respectively. The magnets produce variable flux according to the magnetic wavelength, λ, and vertical displacement, d. The voltages belonging to the coil and phase can be defined as in Eqs. (2) and (3), respectively:

$$v(t) = N\frac{d\phi}{dt}, \tag{2}$$

$$v(t) = \hat{V}\cos(\omega_m t)\cos\left(\frac{\pi d}{\lambda}\sin(\omega_m t) + \theta\right), \tag{3}$$

where $\hat{V}$ is the peak phase to neutral voltage, ω_m is the wave angular frequency, and N is the number of turns

in each coil. The phase voltage involving the wave model can be represented as:

$$v_a(t) = \hat{V}\cos(\omega_m t)\cos\left(\frac{\pi d}{\lambda}\sin(\omega_m t)\right). \tag{4}$$

The stochastic structure of a real sea wave environment involves more than one harmonic frequency while monochromatic sea conditions indicate a single wave envelope-type frequency. However, a monochromatic wave is used as a base to examine and emphasize the effects of the BQE scheme using a fuzzy logic dynamic PI controller on the wave energy system. A set of monochromatic wave travelling parameters representing the sea waves on the coast of Trabzon, Turkey [38] were used in the study.

2.1.2. Laboratory setup for the WECS testing

A reducer and a PMDC motor are used to emulate the wave turbine for producing waving speeds and torque input to a generator shown in Figure 1a. The system parameters are given in the Appendix. The generally known and accepted dynamic model of the PMDC motor and the models belonging to the three-phase permanent magnet generator and reducer are utilized together in simulation to contribute effective realization of the proposed WECS model entirely, and thus the WECS can be tested on the proposed control algorithms by simulation before experimental studies.

2.2. Buck converter

A buck type DC-DC converter, which is a bridge and controlled interface device between the BQE and the load, is used to drive the motor load. The load demand is provided by keeping the voltage at the required magnitude with control of the buck converter. Since information about the buck converter operation can be found in any power electronics book and the initial version of this paper [32], no more details are given here.

2.3. The bus quantity enhancer (BQE)

Concerns arise because of voltage instability, current discontinuity, and power quality, which are affected by AC and DC side voltage and current variations. Irregular behavior of the wave characteristics cause long/short durations in generated voltage, which yields fluctuations in current, frequency, and power [39]. Discontinuity in voltage, current, and power must be eliminated in order to establish a problem-free sustainable power generating unit.

Thus, the BQE shown in Figure 1b is proposed and used to balance the source and load requirements by acting as a green power filter so that the undesired states are eliminated and power consumption is reduced. Discontinuity in sea wave behavior creates higher sags in voltage and currents at the DC bus for each starting moment of the wave cycles. The BQE scheme attenuates discontinuity, fluctuation, ripples, and drops in the voltage and current of the WECS.

In this study, the main focus is to hold the mean value of DC bus voltage constant and to improve the DC bus voltage stabilization with the BQE, whose objective is to ensure power transfer from the DC bus into the load side at regulated voltage and frequency. The BQE transforms and arranges the rectified WECS voltage so that a regulated DC bus voltage is obtained with the control techniques applied. A buck converter is employed to supply power to a PMDC motor load effectively.

There are two operation states of the BQE device as shown in Figure 1b. In State I, the IGBT (S_A) is ON while the IGBT (S_B) is OFF and the diode (D_2) does not allow current to flow, resulting in an increase

in the inductor current. The capacitor keeps the output voltage up constantly during this state. When input voltage is smaller than output voltage, the current flow diagram is indicated as in State I. When input voltage is larger than output voltage, the current flow diagram is shown as in State II where switch S_A is OFF and switch S_B is ON. Therefore, the current flows from inductor L_f to diode D_2, capacitors C_f and C_d, and terminals B_1B_2 and back to the source. The power transfer is accumulated in the capacitor.

The battery and flywheels are two energy storages that are used to fill in the voltage sags caused by the irregular behavior of the waves. The stored energy is used as a compensating power for providing a constant and stable voltage on the DC bus. However, the cost of energy storage is high and it requires regular maintenance. Otherwise, the use of a capacitor presents a solution with no-cost maintenance [40].

The operational characteristics of the BQE scheme are presented by voltage and current waveforms as shown in Figure 1b. As the inductor works during discontinuous mode, the voltage at the output is adjusted at the desired reference level.

3. Multivariable global error driven controller

Controllers are designed to ensure faster and overshoot-free transient responses without or with minimum steady-state error while providing high stability margin, increased productivity, improved quality, and reduced maintenance requirements. Classical (proportional (P), proportional-integral (PI), and proportional-integral-derivative (PID)) control has been used in many different areas with the advancement of control technology, such as modern, optimal, robust, and adaptive control theories. Particularly, classical control is preferred in most process control applications [41,42].

Undesirable effects such as nonlinearities, complicated dynamics, process uncertainty, and varying parameters of the systems decrease the classical controller efficiencies. It is claimed that 80% of classical controller parameters are badly tuned [43]. Adjustment of classical controller parameters can be done with various types of analytical, heuristic, frequency, optimization, and adaptive methods [44]. One of these methods is the fuzzy logic controller (FLC), which is applied in problems where conventional control is not applicable or has limitations such as in systems that include nonlinearity, plant uncertainty, multiple variables, environmental constraints, measurement uncertainties, and temporal behaviors [45–47]. A number of works on the combination of FLCs and classical controllers have been done to enhance the design and performance of both the control stage and the system [48].

Two multierror driven control schemes are utilized in digital simulations and a laboratory validation study here. The aim of the first dynamic error driven control scheme is DC voltage control with a single negative feedback loop, and in the second, an alternative multivariable structure is utilized to contain power and DC current changes in the controller in addition to the control of voltage.

The multivariable structure is used to obtain a dynamic error signal to drive a single controller. Any error in DC voltage magnitude is compensated by the controller using the voltage error path from the multivariable error collecting system, which also includes deviations in current and power. Due to the voltage characteristics of the wave generator, changes occur in generated power causing changes in current as well. Load switching on the load side results in power and current changes, too. These changes in current and power on either generator or load side affect the load bus voltage, which has to be kept constant for the sake of nominal operating conditions of the user load bus. Therefore, the major changes in current and power are included as additional variables in the voltage control algorithm. With the multivariable dynamic error detecting algorithm, any major change in current and power yields a signal to be added to the voltage error, and hence the controller acts to keep

the voltage constant for various operating conditions. Temporary and instantaneous changes such as very short ripples in power are filtered out using a low pass filter and only the major changes are included in the loop as shown in Figure 1c. Since the total error signal is the sum of all global errors determined by the multivariable algorithm, a single controller becomes enough to be used to generate the required switching of the power filter, the BQE. Instead of using separate controllers for each variable, the use of the multivariable dynamic error detecting algorithm with a single controller is more economical and has fast response ability to the changes.

The control scheme for the BQE has a multivariable error driven dynamic structure as described above and shown in Figure 1c. The control algorithm uses three dynamic error driven variables consisting of voltage, current, and power. Therefore, the global error signal is obtained as a weighted sum of the signals coming from these three variables as:

$$e_t = \gamma_v e_v + \gamma_p e_p + \gamma_i e_i, \tag{5}$$

where γ_v, γ_p, and γ_i are the weighting factors for the related variables and their values are obtained by trial and error. The variable error signals e_v, e_p, and e_i are the voltage, power, and current errors, respectively, and are defined as follows:

$$e_v = v_{dr} - v_d, \tag{6}$$

where v_{dr} and v_d are reference and BQE output DC voltages in pu, respectively. The power error signal is defined as the major change in power as:

$$e_p = p_0(k) - p_0(k-1), \tag{7}$$

where k is an iteration counter and

$$p_0(k) = \frac{1}{1+sT_0} p_i(k), \tag{8}$$

where p_i is the active power in pu obtained as the product of pu voltage v_d and pu current i_d. The parameter T_0 is the low pass filter time constant used in Eq. (8). The low pass filter with time constant T_0 is used to exclude temporary and instantaneous changes such as short ripples in power and includes only the major changes with long durations in the total error signal given in Eq. (5).

The current error signal is represented by the change in current as:

$$e_i = i_d(k) - i_d(k-1). \tag{9}$$

Adding the change in current as the current error signal to the error variables enables the algorithm to generate an additional error signal whenever the value of the DC current changes due to load switching and wave effects.

The inclusion of power and current error variables to generate a multivariable dynamic error signal in the DC voltage control algorithm improves the stability and ensures a reliable voltage magnitude for load bus.

The total error, e_t, of the multierror variable form goes into the adaptive fuzzy tuned PI (AFTPI) controller block shown in Figure 1c. In this figure, $e(k)$ is the dynamic error at the kth sampling. The change in error is defined as:

$$de(k) = e(k) - e(k-1). \tag{10}$$

The FLC is designed to tune the parameters (K_P and K_I) of the PI controller online as the system operates. Since a classical PI controller has constant parameters set at the beginning and used during operation, it sometimes fails to handle the effects of the changes in system parameters and different operating conditions. Therefore, as shown in Figure 1c, the FLC is combined with the PI controller to tune its parameters to the

best applicable values suited for the current operating condition. Proportional gain parameter K_P is chosen in interval [K_{Pmin}, K_{Pmax}] such that the controller performs better. Similarly, the integral gain parameter is selected in interval [K_{Imin}, K_{Imax}]. These upper and lower limits of the PI controller are chosen as the parameter boundaries considering the bounded input bounded output (BIBO) stable operating conditions of the system. The BIBO stability of the system is tested by observing the output when step type reference voltage input is applied to the system. The FLC is then used to tune the parameters K_P and K_I of the PI controller so that the steady-state voltage error is minimum. Therefore, with this control error minimization-based tuning process, the classical PI controller turns into an AFTPIC. The FLC has the classical structure and comprises three main parts, namely the fuzzifier, rule base, and defuzzifier, as shown in Figure 1c.

The FLC inputs are error, e, and change in error, de. Five membership functions are used to convert the input signals to fuzzy subsets first in the fuzzifier stage. Triangle-shaped fuzzy membership functions are employed in this study since they are modeled easily due to their linearity and they require less time and memory in control algorithms. The fuzzified values of e and de are then applied in the table of rules given in Table 1 to obtain the fuzzy number.

Table 1. Fuzzy logic rules decision table for FLCs.

		$\dot{e}$				
		NB	NS	ZZ	PS	PB
e	NB	S	S	M	M	B
	NS	S	M	M	B	VB
	ZZ	M	M	B	VB	VB
	PS	M	B	VB	VB	VVB
	PB	B	VB	VB	VVB	VVB

Although a rule table is one of the most important parts in building a fuzzy system, there is no generally effective and efficient accepted method to design a fuzzy rule table [49,50]. Two techniques based on the direct knowledge from experts and the automatic knowledge from numerical data have been used to achieve this task [49,51]. The rule table used in this study is generated using the system response approach given in [52] where a symmetrical rule table is derived based on the idea discussed in [53]. The central of area (COA) defuzzifier scheme is used to acquire the crisp values through the resultant united fuzzy subsets representing the controller output. A trial and error method is used to determine the FLC parameters.

The MATLAB/Simulink environment is used to develop the FLC addressed here as a universal control tool. It lets users easily change its parameters so that it can be applied to control systems having different characteristics. Further information about the FLC used here can be found in [52].

A pulse generator is driven by the controller output signal to modulate pulses so that converter switching signals S_A and S_B are generated where $S_B = not(S_A)$.

4. MATLAB/Simulink digital simulation

The WECS scheme is modeled in the MATLAB/Simulink environment and simulated for different operating scenarios so that the evaluation of system performance can be realized. The system simulation block diagram constituted by using the operational dynamic blocks in the MATLAB SimPowerSystems library is shown in Figure 2. The values of system components such as capacitors, diodes, and the other semiconductors are set to the same values referred to in the datasheets. The parameters of the system used for simulation are given in the Appendix.

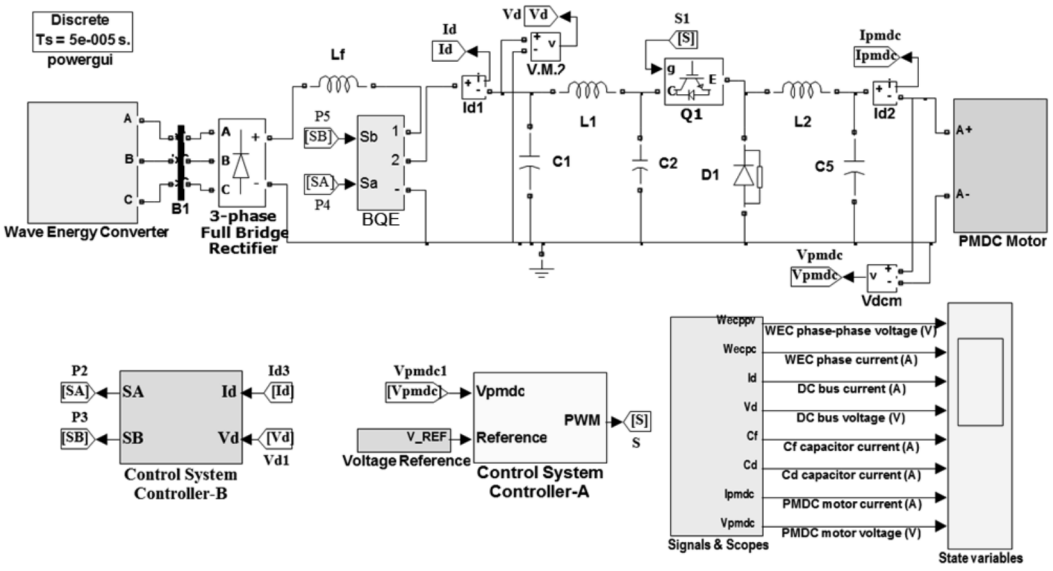

Figure 2. The simulation block model of the system with the BQE.

5. Laboratory prototype implementation

The unified system Simulink model is run in real time and interfaced with power electronics devices by means of the Real-Time Windows Target accessible in the MATLAB environment, which makes it possible to compose and control real time executable commands for applications in real time through MATLAB [54,55].

In this study, a PCI-6070E DAQ card is used to build communication on data acquisition between the real time part and the computer, which contains the digital system model. The features of the DAQ card are given in the Appendix.

The main control units of the AC/DC system with and without the FACTS-based BQE filter are modeled in MATLAB/Simulink. Since the active rectifier needs at least one controllable active switching semiconductor along with passive switches and components, a passive rectifier is preferred in order to provide cost reduction and less controller difficulty, improving robustness in the output voltage. The WEC emulator output is rectified by a three-phase full-wave uncontrolled bridge rectifier and is then applied to the converter without the BQE scheme.

6. Simulation and experimental results

The laboratory setup for experiments shown in Figure 3 consists of the data acquisition system with three voltage and five current sensors, and an analog input board. The system parameters used for testing by both simulation and experiment are given in the Appendix. An experimental test setup has been arranged to verify the models of simulation for the proposed converters and control algorithms as shown in Figure 3. In simulation and experimental works, the system is observed under two different cases tabulated in Table 2.

Under the operating condition, in which the wave period is increased, it is observed that the generated voltage waveform includes less discontinuity. On the other hand, if the wave period is decreased as another operating condition, it is seen that voltage sags and swells increase, resulting in lower system performance. The wave period without the BQE scheme is taken as longer than with the BQE scheme to indicate the effectiveness of the filtered control system. The system with the BQE scheme is tested for the worst cases. For example,

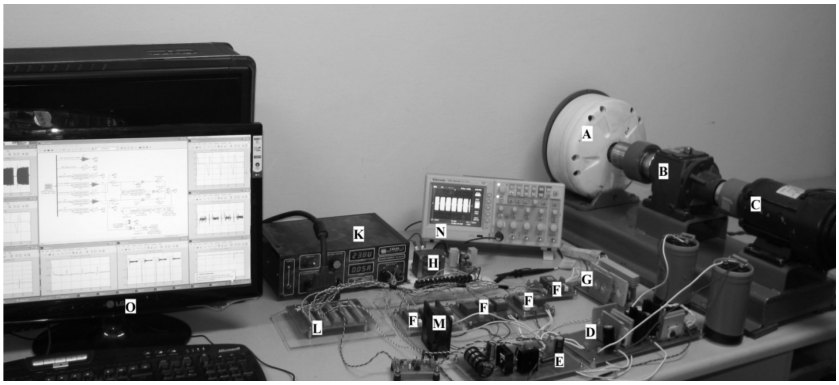

Figure 3. Experimental setup. A: Generator; B: reducer; C: PMDC motor; D: BQE circuit; E: converter; F: sensors; G: rectifier; H: DC supply (sensors); K: DC supply (BQE and converter circuits); L: DAQ card connector; M: load; N: scope; O: PC.

Table 2. The two different system scenarios for the real time experimental studies.

	Case I	Case II
PMDC motor voltage trajectory tracking reference (V_{mr})	Variable	Variable
DC bus reference voltage (V_{dr})	20 V	20 V
BQE model	Without	With

when the results under the operating conditions are considered in this study here with those of [33], in which only a PI controller with constant parameters is used without any tuning, it is observed that the duration of the continuity with PI is only 5.712 s and the duration of discontinuity is 1.571 s. On the other hand, the durations of continuity and discontinuity with the fuzzy tuned PI of this study are 3.37 and 1.645 s, respectively. It means that the ratio of continuity to discontinuity is $5.712/1.571 = 3.636$ when only the PI controller is used, and it is $3.37/1.645 = 2.04$ when the fuzzy tuned PI controller is used. The higher ratio means that more kinetic energy is stored in a rotating mass to be dissipated during discontinuity. Therefore, the voltage sags are expected to be less under the operating condition with the higher ratio, in which only the PI controller was used, and the voltage sags are expected to be higher with the lower ratio operating condition when the fuzzy tuned PI is used. Since the sags are almost the same from both controllers, we conclude that the fuzzy tuned PI works better since it yields almost the same results under more difficult operating conditions.

Error energy-based performance measures such as ISE, IAE, and ITAE are used to compare the performances of the controllers in terms of parameter optimization. To realize a satisfying comparison between the controllers, IAE and ITAE are used to get information about operational characteristics of the controllers during transient and steady-state operation. Since the information about the error energy-based performance indices can be found in any optimal control book, no details are given here.

The AC/DC system performance for Cases I and II are given in Figures 4–6. In these cases, the load operation with a variable voltage reference is discussed. The load voltage is changeable for these scenarios so that the load reference voltage is applied in a series of steps to discuss the performance of the buck converter.

The resulting waveforms obtained from experiment and simulation works without and with the BQE are represented in the same figures to provide an effective comparison and show the BQE's impact on performance. The WEC output voltage waveform is shown in Figure 4; while the peak values of the WEC voltages are below

21 V without the BQE, they are above 21 V with the BQE. Similar voltage waveforms are recorded from simulations and experiments as shown in Figure 4. The WEC voltage is kept constant as the DC load voltage with step changes as shown in Figure 6.

The DC bus voltage usually encounters variations and sudden step changes. The novel FACTS-based BQE is applied to keep the common DC bus voltage constant at 20 V as shown in Figure 5. It can be seen from Figures 5 and 6 that the convergence of the DC bus voltage is ensured with minimum DC voltage variations, where the DC common bus voltage is stabilized when the DC load voltage is lower or higher than the reference value (20 V). The BQE system controller performances have been determined by the means of ISE, IAE, and ITAE as given in Tables 3 and 4. Improvement is observed in the system performance.

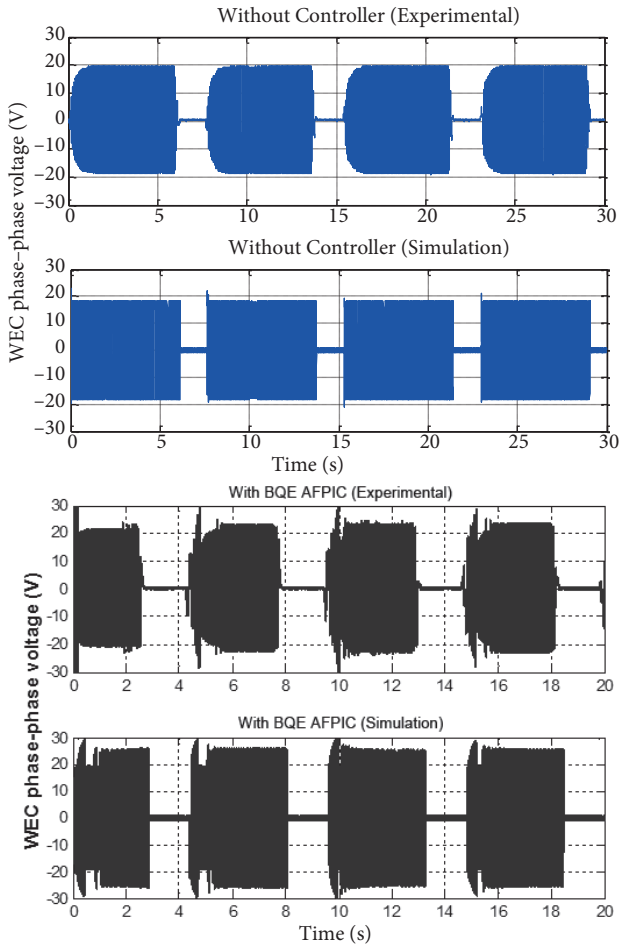

Figure 4. WEC phase-phase voltage.

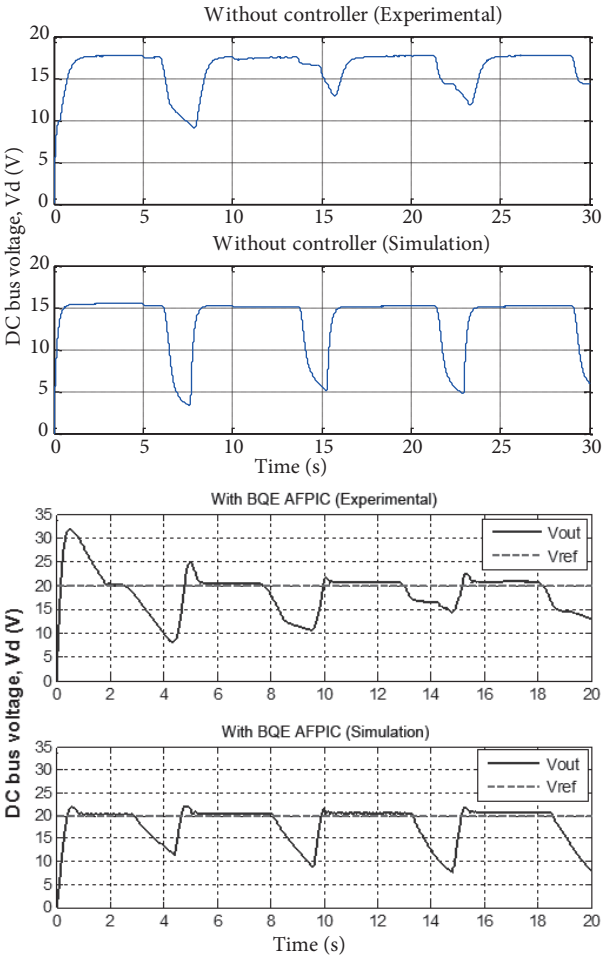

Figure 5. DC bus voltage (V_d).

Table 3. DC bus voltage under variable voltage control.

Filter	Controller	Method	ISE	IAE	ITAE
None	None	Experiment	576.8663	112.0012	1583.1871
		Simulation	1572.4872	192.6991	2929.0777
BQE	AFPIC	Experiment	436.3712	65.3647	553.2747
		Simulation	391.8645	53.6663	589.4391

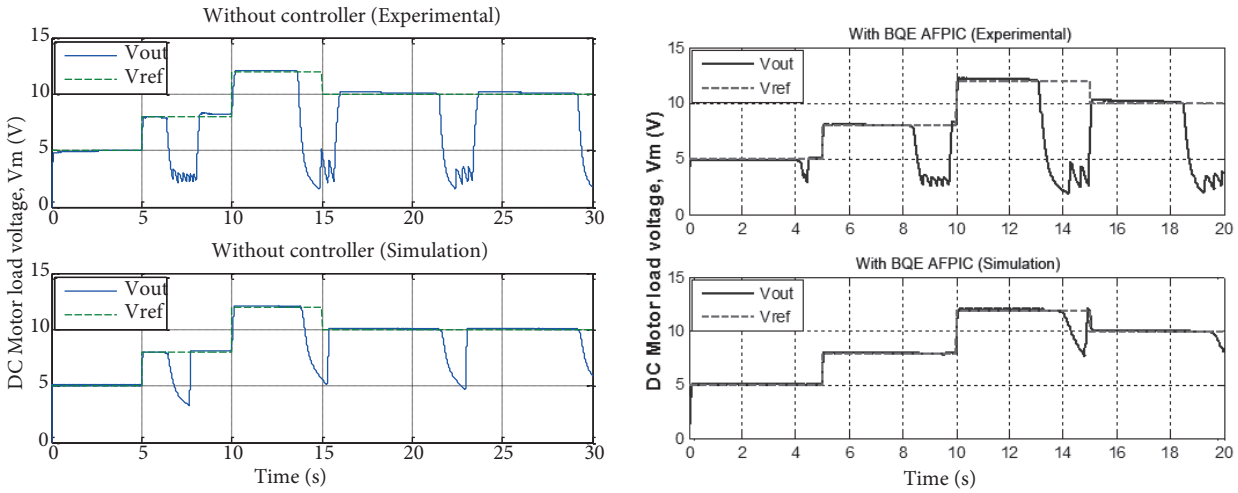

Figure 6. PMDC motor voltage (V_m).

Table 4. PMDC motor load voltage under variable voltage control.

Filter	Controller	Method	ISE	IAE	ITAE
None	None	Experiment	301.4509	46.1923	792.2616
		Simulation	76.0245	19.5800	318.9888
BQE	AFPIC	Experiment	224.7212	33.4801	479.1973
		Simulation	8.9981	4.3074	52.8773

7. Conclusion

A novel FACTS-based switched power filter scheme that can be called a BQE is designed and regulated by a multivariable dynamic error driven fuzzy logic tuned PI controller in order to stabilize the wave energy system operating as a standalone source for DC loads.

In the scheme without the BQE, the WECS output AC voltage is rectified and employed to the DC-DC converter. The converter is then controlled to meet DC load demands. The purpose of using the novel adaptive fuzzy PI controlled BQE device is to provide a stable DC bus voltage regulation. It is shown that the proposed adaptive fuzzy PI used in the BQE scheme improved the DC bus voltage stabilization so that energy utilization is enhanced (Figure 5). The use of the multivariable control strategy enables the regulating system to react to any variations in load power and current to form the required control acts for a constant DC bus voltage (Figure 5). The FACTS BQE scheme regulated by the time-descaled dynamic error variables and the AFPIC is the main contribution of this study, ensuring the necessary DC bus voltage stabilization. The proposed scheme and the controller are validated using the developed MATLAB simulation model of the unified AC/DC system and comparison was made with those acquired from the experiment test setup of the same system to validate the model. It can be inferred from the comparison of the results for test scenarios that the application of the adaptive fuzzy PI controlled BQE scheme and the multivariable error driven fuzzy logic control approach provides a mean constant DC bus voltage (Figure 5) for the variable load voltage trajectory test case (Figure 6). This problem can be figured out without difficulty just using a backup battery storage system such that the load demand is operated effectively from the battery during the beginning of each wave cycle. Since the worst case scenario is dealt with here, the constructive support of any battery storage scheme is not considered. Even without the use of an expensive backup battery storage scheme, the magnitudes of the DC bus voltage

fluctuations are reduced.

The same flexible and adaptive fuzzy logic PI controlled FACTS BQE scheme can be extended to other AC/DC interface schemes using wind-photovoltaic systems, wave-micro-hydro, and other integrated AC/DC hybrid green power systems. Other control methods in terms of artificial intelligence and soft-computing controllers can also be used.

Nomenclature

L_f	DC bus filter inductance
C_f	DC bus filter capacitor
I_d	DC bus current
V_d	DC bus voltage
I_m	DC motor current
V_m	DC motor voltage
L_m	DC motor inductance
R_m	DC motor resistance
J	DC motor nonlinear inertia
B	DC motor friction
K_T	DC motor torque constant
e_m	DC motor voltage error signal
γ_i	Current loop weight gain
γ_v	Voltage loop weight gain
γ_p	Power loop weight gain
de	Error variation
e	Error
C_d	BQE capacitor
D_2	BQE freewheeling diode
T_o	Low pass filter time delay
$\hat{V}$	Peak phase-neutral
N	Number of turns per coil
v_{dr}	DC motor reference voltage

References

[1] Bose BK. Global warming; energy, environmental pollution, and the impact of power electronics. IEEE Ind Electron M 2010; 4: 6-17.

[2] Saidur R, Atabani AE, Mekhilef S. A review on electrical and thermal energy for industries. Renew Sust Energ Rev 2011; 15: 2073-2086.

[3] Wang L, Chen ZJ. Stability analysis of a wave-energy conversion system containing a grid-connected induction generator driven by a wells turbine. IEEE T Energy Conver 2010; 25: 555-563.

[4] Sharaf AM, Wang W, Altas IH. A novel hybrid active filter compensator for stabilization of wind-utility grid interface scheme. Eur T Electr Power 2010; 20: 306-326.

[5] Altas IH, Sharaf AM. A novel on-line MPP search algorithm for PV arrays. IEEE T Energy Conver 1996; 11: 748-754.

[6] Bull SR. Renewable energy today and tomorrow. P IEEE 2001; 89: 1216-1226.

[7] Blaabjerg F, Iov F, Kerekes T, Teodorescu R. Trends in power electronics and control of renewable energy systems. In: 14th International Power Electronics and Motion Control Conference (EPE/PEMC 2010); 6–8 September 2010; Ohrid, Macedonia. New York, NY, USA: IEEE. pp. K-1-K-19.

[8] Lenee-Bluhm P, Paasch R, Ozkan-Haller HT. Characterizing the wave energy resource of the US Pacific Northwest. Renew Energ 2011; 36: 2106-2119.

[9] Rahm M, Bostrom C, Svensson O, Grabbe M, Bulow F, Leijon M. Offshore underwater substation for wave energy converter arrays. IET Renew Power Gen 2010; 4: 602-612.

[10] Muetze A, Vining JG. Ocean wave energy conversion-a survey. In: 2006 IEEE Industry Applications Conference Forty-First IAS Annual Meeting; 8–12 October 2006; Tampa, FL, USA. New York, NY, USA: IEEE. pp. 1410-1417.

[11] Ruellan M, BenAhmed H, Multon B, Josset C, Babarit A, Clement A. Design methodology for a SEAREV wave energy converter. IEEE T Energy Conver 2010; 25: 760-767.

[12] Lindroth S, Leijon M. Offshore wave power measurements-a review. Renew Sust Energ Rev 2011; 15: 4274-4285.

[13] Wang SJ, Yuan P, Li D, Jiao YH. An overview of ocean renewable energy in China. Renew Sust Energ Rev 2011; 15: 91-111.

[14] Falco AFD. Wave energy utilization: a review of the technologies. Renew Sust Energ Rev 2010; 14: 899-918.

[15] Drew B, Plummer AR, Sahinkaya MN. A review of wave energy converter technology. P I Mech Eng A-J Pow 2009; 223: 887-902.

[16] O'Sullivan D, Griffiths J, Egan MG, Lewis AW. Development of an electrical power take off system for a sea-test scaled offshore wave energy device. Renew Energ 2011; 36: 1236-1244.

[17] Tedeschi E, Carraro M, Molinas M, Mattavelli P. Effect of control strategies and power take-off efficiency on the power capture from sea waves. IEEE T Energy Conver 2011; 26: 1088-1098.

[18] Amon E, Brekken TKA, von Jouanne A. A power analysis and data acquisition system for ocean wave energy device testing. Renew Energ 2011; 36: 1922-1930.

[19] Piasecki S, Jasinski M, Rafal K, Korzeniewski M, Milicua A. Higher harmonics compensation in grid-connected PWM converters for renewable energy interface and active filtering. Prz Elektrotechniczn 2011; 87: 85-90.

[20] Barnes M, El-Feres R, Kromlides S, Arulampalam A. Power quality improvement for wave energy converters using a D-STATCOM with real energy storage. In: 2004 1st International Conference on Power Electronics Systems and Applications; 9–11 November 2004; Hong Kong. Kowloon, Hong Kong: Hong Kong Polytechnic University. pp. 72-77.

[21] Amon EA, Schacher AA, Brekken TKA. A novel maximum power point tracking algorithm for ocean wave energy devices. In: 2009 IEEE Energy Conversion Congress and Exposition; 20–24 September 2009; San Jose, CA, USA. New York, NY, USA: IEEE. pp. 2635-2641.

[22] Blanco M, Navarro G, Lafoz M. Control of power electronics driving a switched reluctance linear generator in wave energy applications. In: 13th European Conference on Power Electronics and Applications (EPE 2009); 8–10 September 2009; Barcelona, Spain. New York, NY, USA: IEEE. pp. 1-9.

[23] Bostrom C, Leijon M. Operation analysis of a wave energy converter under different load conditions. IET Renew Power Gen 2011; 5: 245-250.

[24] Xiang J, Brooking PRM, Mueller MA. Control requirements of direct drive wave energy converters. In: 2002 IEEE Region 10 Technical Conference on Computers, Communications, Control and Power Engineering; 28–31 October 2002; Beijing, China. New York, NY, USA: IEEE. pp. 2053-2056.

[25] Bostrom C, Lejerskog E, Tyrberg S, Svensson O, Waters R, Savin A, Bolund B, Eriksson M, Leijon M. Experimental results from an offshore wave energy converter. J Offshore Mech Arct 2010; 132: 041103-1/041103-5.

[26] Thorburn K, Bernhoff H, Leijon M. Wave energy transmission system concepts for linear generator arrays. Ocean Eng 2004; 31: 1339-1349.

[27] Igic P, Zhou Z, Knapp W, MacEnri W, Sorensen HC, Friis-Madsen E. Multi-megawatt offshore wave energy converters-electrical system configuration and generator control strategy. IET Renew Power Gen 2010; 5: 10-17.

[28] Lopes MFP, Henriques JCC, Lopes MC, Gato LMC, Dente A. Design of a non-linear power take-off simulator for model testing of rotating wave energy devices. In: 8th European Wave and Tidal Energy Conference; 7–10 September 2009; Uppsala, Sweden. Uppsala, Sweden: Uppsala University. pp. 715-721.

[29] Kuo JL, Chao KL. Grid-connected multilevel inverter with intelligent petri nets controller for ocean current power generation system. Int Rev Electr Eng-I 2010; 5: 858-869.

[30] Hals J, Falnes J, Moan T. Constrained optimal control of a heaving buoy wave-energy converter. J Offshore Mech Arct 2011; 133: 011401-1/011401-15.

[31] Ozkop E, Altas IH, Sharaf AM. A novel fuzzy logic tansigmoid controller for wave energy converter-grid interface dc energy utilization farm. In: IEEE Canadian Conference on Electrical and Computer Engineering, 2009; 3–6 May 2009; St. Johns, Canada. New York, NY, USA: IEEE. pp. 1184-1187.

[32] Ozkop E, Altas IH, Sharaf AM. A novel switched power filter-green plug (SPF-GP) scheme for wave energy systems. Renew Energ 2012; 44: 340-358.

[33] Sharaf AM, El-Gammal, AAA. Novel low cost green plug smart filter soft starter (GP-SF-SS) schemes for small horse power motorized loads. Int J Elec Power Eng 2010; 4: 113-146.

[34] Shek JKH, Macpherson DE, Mueller MA, Xiang J. Reaction force control of a linear electrical generator for direct drive wave energy conversion. IET Renew Power Gen 2007; 1: 17-24.

[35] Pinto FT, Silva R. Specific kinetic energy concept for regular waves. Ocean Eng 2006; 33: 1283-1298.

[36] Sorensen RM. Basic Coastal Engineering. 3rd ed. New York, NY, USA: Springer, 2006.

[37] Brooke J. Wave Energy Conversion. 1st ed. Oxford, UK: Elsevier, 2003.

[38] Sağlam M. Calculating the technical potential of wave energy in Turkey, case studies for project feasibility and design. MSc, Marmara University, İstanbul, Turkey, 2004.

[39] Granados-Lieberman D, Romero-Troncoso RJ, Osornio-Rios RA, Garcia-Perez A, Cabal-Yepez E. Techniques and methodologies for power quality analysis and disturbances classification in power systems: a review. IET Gener Transm Dis 2011; 5: 519-529.

[40] Brooking PRM, Mueller MA. Power conditioning of the output from a linear vernier hybrid permanent magnet generator for use in direct drive wave energy converters. IEE P-Gener Transm D 2005; 152: 673-681.

[41] Da Z, Zhengyun R, Jian'an F, Lei, J. Computation of stabilizing PI and PID controllers by using Kronecker summation method. In: 27th Chinese Control Conference; 16–18 July 2008; Kunming, China. Beijing, China: Beijing University of Aeronautics & Astronautics. pp. 72-75.

[42] Yu CC. Autotuning of PID Controllers: A Relay Feedback Approach. 2nd ed. Berlin, Germany: Springer-Verlag, 2006.

[43] O'Dwyer A. Handbook of PI and PID Controller Tuning Rules. London, UK: Imperial College, 2009.

[44] Panda RC, Yu CC, Huang HP. PID tuning rules for SOPDT systems: review and some new results. ISA T 2004; 43: 283-295.

[45] Kalogirou SA. Artificial intelligence for the modeling and control of combustion processes: a review. Prog Energ Combust 2003; 29: 515-566.

[46] Monmasson E, Cirstea MN. Fpga design methodology for industrial control systems-a review. IEEE T Ind Electron 2007; 54: 1824-1842.

[47] Gupta RA, Kumar R, Bansal AK. Artificial intelligence applications in permanent magnet brushless dc motor drives. Artif Intell Rev 2010; 33: 175-186.

[48] Mann GKI, Hu B, Gosine RG, Analysis of direct action fuzzy PID controller structures. IEEE T Syst Man Cy B 1999; 29: 371-388.

[49] Castro PAD, Camargo HA. Learning and optimization of fuzzy rule base by means of self-adaptive genetic algorithm. In: 2004 IEEE International Conference on Fuzzy Systems; 25–29 July 2004; Budapest, Hungary. New York, NY, USA: IEEE. pp. 1037-1042.

[50] Yam Y, Baranyi P, Yang CT. Reduction of fuzzy rule base via singular value decomposition. IEEE T Fuzzy Syst 1999; 7: 120-132.

[51] Li HX, Gatland HB. New methodology for designing a fuzzy logic controller. IEEE T Syst Man Cy 1995; 25: 505-512.

[52] Altas IH, Sharaf AM. A generalized direct approach for designing fuzzy logic controllers in MATLAB/Simulink GUI environment. Int J Inform T Intell Comput 2007; 1.

[53] MacVicar-Whelan PJ. Fuzzy sets for man-machine interaction. Int J Man Mach Stud 1976; 8: 687-697.

[54] Miao L, Zou G, Shi P, Jiao X. Development of hardware driver for MATLAB/Simulink real-time simulation. In: International Workshop on Intelligent Systems and Applications; 23–24 May 2009; Wuhan, China. New York, NY, USA: IEEE. pp. 1-4.

[55] Teng FC. Real-time control using MATLAB Simulink. In: IEEE International Conference on Systems, Man and Cybernetics; 8–11 October 2000; Nashville, TN, USA. New York, NY, USA: IEEE. pp. 2697-2702.

Appendix

System and control parameters

PMDC motor	
Power (W)	250
Voltage (V)	24
Current (A)	12
Speed (rpm)	1500
Speed reducer	
Power (W)	370
Conversion	4
Speed (rpm)	359
Moment (Nm)	9.4
WEC (simulation)	
Three-phase source	
Voltage (V)	13.5
Phase angle (degrees)	0
Frequency (Hz)	21
Connection	Star
Short-circuit level (VA)	1250
Base voltage	30
X/R ratio	5
System with the BQE (MATLAB/Simulink)	
BQE system	
$C_d(F)$	34,000 u
The switched S_A, S_B	
$R_{on}(\Omega)$	0.001
$R_s(\Omega)$	100
$C_s(F)$	10 n
Rectifier (1-phase & 3-phase)	
$R_s(\Omega)$	100 k
$C_s(F)$	Inf
Diode	
$R_{on} = 1\,m\Omega,\ L_{on} = 0\,H,\ V_f = 1.5\,V$	
Controller-A (buck converter)	
PI controller parameters	
$K_{P(Vm)} = 3,\ K_{I(Vm)} = 1$	
PWM generator	
Frequency (Hz)	1000
Sampling (s)	50 u
Controller-B (BQE)	
The loop weight gain	
$\gamma_i = 0.1,\ \gamma_v = 1,\ \gamma_p = 0.1$	
PWM generator	
Frequency (Hz)	1000
Sampling (s)	50 u

Generator	
Power (W)	1500
Speed (rpm)	550
Moment (Nm)	35
Resistance (Ω)	5
Inductance (mH)	18.2
Pole number	8
Generator arrangement	Star
The DAQ card	
AI	16SE / 8DI
Resolution	12 bits
Sampling (max.)	1.25 MS/s
AO	2
Output Rate	1 MS/s
Dig. I/O	8
Timer/Counter	24, 2-bit
PDMC motor (simulation)	
$L_m(H)$	0.0805
$R_m(\Omega)$	42
$J\left(\mathrm{Nm/rad/s^2}\right)$	0.2 m
$B\left(\mathrm{Nm/rad/s}\right)$	30 u
$K_T\left(\mathrm{Nm/A}\right)$	80 m
$K_{emf}\left(V/rad/s\right)$	80 m
DC bus filter	
$L_f(H)$	9.5 u
$C_f(F)$	4700 u
Buck converter	
$C_1(F)$	10 u
$L_1(H)$	10.16 u
$C_2(F)$	10 u
Diode (D1)	
$R_s(\Omega)$	100
$C_s(F)$	10 n
$R_{on} = 1\,m\Omega,\ L_{on} = 0\,H,\ V_f = 1.8\,V$	
Buck converter switch Q1 (IGBT)	
$R_{on}(\Omega)$	0.001
$R_s(\Omega)$	100
$C_s(F)$	10 n
Buck converter filter	
$L_2(H)$	32.4 u
$C_5(F)$	100 u